International Journal of Water Resources and Arid Environments 9(2): 123-133, 2020
ISSN 2079-7079

Hydroxyapatite / Chitosan Nanocomposite Materials as Potential Adsorbent for Cr Removal From Aqueous Solution

Safaa M. Ragheb, Nouran Y. Mohamed and Mohamed S. Mahmoud

Housing of Building, National Research Center, Egypt

Abstract: Hydroxyapatite (HAP) is a possible sorbent for heavy metals in wastewater due to its high adsorption capacity and low water solubility. In the present study, the potential of synthesized hydroxyapatite / chitosan (HAPCs) composite to remove chromium (VI) from aqueous solutions was investigated by batch tests under different experimental conditions. The chemical and morphological structures of adsorbent were investigated by scanning electron microscopy (SEM), energy dispersive analysis of X-rays (EDAX), element analyzer and Fourier-transform infrared spectroscopy (FTIR). The study also investigated the effects of process parameters such as initial Cr(VI) concentration, solution pH and contact time . Results of the present study revealed that the adsorption rate was very high in the beginning and over 94% of Cr(VI) removal was achieved within the first 5 min. At pH < 7 and >5, the overall Cr(VI) adsorption mechanism can be described to follow four different steps namely, (i) strong electrostatic interaction between positively charged adsorbent surface and negatively charged adsorbate in the aqueous solution, (ii) electrostatic attraction between positively charged adsorbent surface hydroxyl group and adsorbate, (iii) ligand or ion-exchange reaction between positively charged adsorbent surface and adsorbate and (iv) dissolution-precipitation. The thermodynamics of Cr(VI) onto HAPCs indicates spontaneous and endothermic nature of the process. Chromium(VI) uptake was quantitatively evaluated using the Langmuir and Freundlich isotherms models. The adsorption equilibrium data was well described by the Langmuir isotherm model with maximum adsorption capacity of 2.208 mmol/g of Cr(VI) ions on HAPCs..

Key words: Hydroxyapatite · Chromium · Adsorption isotherm · Chitosan

INTRODUCTION

Chromium(VI) has been considered as one of the top 16 toxic pollutants because of its carcinogenic and tetratogenic characteristics. For this reason, it has become a serious public health concern, with the World Health Organization specifying its tolerance limit as 0.05 mg/ [1]. Chromium can be released into the environment through a large number of industrial operations including those of the metal-finishing industry, chromium and steel industries and inorganic chemical production. The extensive use of chromium results in the generation of large quantities of chromium-containing effluents which require an exigent treatment. Hexavalent chromium species are strong oxidants that exist in water as oxyanions such as chromate $HCrO_4^-$ and dichromate $Cr_2O_7^{-2}$. The environmental remediation of Cr(VI) usually involves the reduction of Cr(VI) ions to the less mobile and less toxic Cr(III) species. However, these methods are not economical on a large scale and have many disadvantages such as incomplete metal removal, the use of expensive reagents and the generation of toxic sludge or other waste products that require disposal or treatment.

In contrast, These toxic metal ions, even at low concentrations, have deteriorated water resources and drinking water and easily accumulated in the human body throughout the food chain, causing a variety of diseases and disorders [2]. So, it is necessary to remove these metal ions from industrial effluents for their subsequent safe disposal. The removal of heavy metal ions from wastewaters has been a subject of extensive industrial research. At the same time, some of them (e.g., Pt and Au) are precious and can be recycled and reused for extensive applications [3, 4]. The recovery of heavy or valuable metals from water or wastewaters can often result in considerable cost savings and have both ecological and economic benefits. Different methods, such as precipitation [5], solvent extraction [6] chemical and

Corresponding Author: Safaa M. Ragheb, Housing of Building, National Research Center, Egypt

electrochemical techniques [7], ion-exchange methods [8] ultrafiltration [9, 10] and reverse osmosis [11, 12], flotation [13] and coagulation [14] have been developed for the removal of toxic metal ions from industrial effluents and wastewaters. However, most of these processes are unacceptable, owing to the disposal of sludge, their high cost, low efficiency and inapplicability to a wide range of pollutants [15].

Adsorption is a well-known separation method and recognized as one of efficient and economic methods for water decontamination applications. In addition, owing to the reversible nature of most adsorption processes, the adsorbents can be regenerated by suitable desorption processes for multiple uses [16] and many desorption processes are of low maintenance cost, high efficiency and ease of operation [17].However, the major problem in this field is to select novel types of adsorbents. A number of adsorbents such as activated carbon [18], zeolites [19, 20], clays [21, 22] chitosan, apatite and agricultural residues [23-25] have been used for the removal of heavy metal ions. Nevertheless the apatite family has demonstrate an ideal and effective sorption capacity .

Hydroxyapatite (HAP), is a member of the apatite family , is a slightly alkaline substance with good biocompatibility also is in good harmony with the environment and will hardly cause secondary pollution. It is a well established fact that the Human bone consists of 20% of collegen fibrils, 69% of nano size crystalline inorganic phase and 9% of water. These Nanosized crystalline composite ingredients mainly resemble hydroxyapatite (HAP) - $Ca_{10}(PO_4)_2(OH)_2$basically a type of calcium phosphate, with structural dimensions similar to a rod or a needle (length 40-60 nm, width 10-20 nm and thickness 1-3 nm). The chemical, structural and morphological properties of HAP bioceramic are highly sensitive to change in physical properties, chemical composition and processing temperature .Since the 1990s, artificial synthesis methods for HAP preparation have increased; such strategies mainly include natural combustion method [26, 27] hydrothermal method [28] sol-gel method [22, 29] Co-Precipitation Method, Microwave Irradiation Method, Mechano Chemical Methodand ultrasonic method [30, 31] Several attempts have been reported using sol gel method for the preparation of HAP. In the sol gel method an organic solvent is used as an alternative to water for the reaction between the reactants. This has the advantages of faster rate of precipitation and solvent evaporation compared with aqueous based systems. In addition, the degree of agglomeration between nano-sized particles is less in organic solvent than aqueous based system [32].This may be related to lower capillary forces between particles and weaker hydrogen bonding in ethanol system compared to that in water.

The basic principle of sol-gel method is that active monomers are produced through hydrolysis reaction of metal alkoxides or inorganic salts. Next, polymerization and gelling of solute are implemented, followed by gel drying and roasting. Finally, inorganic nanomaterial is gained. Particles prepared by sol-gel method have good chemical homogeneity, high purity and small size. Moreover, this method accommodates indissolvable or insoluble components and dried gel particles that have low sintering temperature. Nevertheless, this method has some shortcomings, such as poor sinterability between gel particles as well as poor sinterability and remarkable shrinkage upon drying of bulk material.

Kuriakose prepared nanocrystalline HAP from organic solvent systems using the sol gel method to promote the characteristics of HAP [33]. The sol gel method can be used to synthesize a pure nano crystalline HAP at 85°C at alkaline pH followed by post processing by sintering at 1200°C. The particle size and shape of HAP fabricated by this method was not reported. Yanji Zang used a very similar method where aqueous solution of $(NH_4)_2HPO_4$ was added to $Ca(NO_3)_2$ ethanol solution. Single phase nanocrystalline HAP was precipitated, while the morphology was changed from spherical to rod shape when the temperature was increased from 40°C to 80°C
in the slow addition mode. However, at 80 °C, spherical particles were formed by the rapid addition mode [34].

Daiwon Choi [35] reported a room temperature process for the fabrication of HAP using organic solvent such as tetrahydrofuran. Spherical HAP particles were formed with diameter between 1 and 10 mm using tetrahydrfuran. The aim of this study was therefore to investigate the feasibility of fabricating nano-size and needle-like shape HAP crystals at low temperature, mimicking the morphology and size of bone apatite crystals.

The main objective of this study is to examine the potential use of HAP as an effective adsorbent in the removal of Cr(VI) ions from synthetic solutions. The adsorption capacities of the composites were evaluated by studying the corresponding equilibrium adsorption isotherms of Cr(VI) ions employing a batch mode. Furthermore, various conditions such as pH, time, temperature and the effect of co-ions were optimized to achieve a maximum sorption capacity.

MATERIALS AND METHODS

Materials: All other chemicals employed were of analytical grade and used without further purification treatment . chitosan (85% de-acetylated) were supplied by sigma-Aldrich. Potassium dichromate, calcium nitrate, ammonium dihydrogen phosphate and ammonia were purchased from Merck (Germany).

Synthesis of n-HAp and n-HAp/Chitosan Composites: n-HAp was synthesized by the reaction of calcium nitrate and ammonium dihydrogen phosphate at a stoichiometric Ca/P ratio of 1.67, with the pH value during mixing being maintained above 10 by the addition of ammonia solution. The resulting precipitate was rinsed with water until the wash water was neutral and then dried at 80°C [36, 37]. The corresponding n-HAp/chitosan composites was also prepared by the precipitation method. Thus, an aqueous solution of ammonium dihydrogen phosphate was added to an aqueous solution containing 3 g of $Ca(NO_3)_2$ and 2 g of chitosan to obtain n-HAp/chitosan /n-HApCs. In both cases, the precipitate formed was rinsed with water to reduce the pH level to a value of 7. The precipitate obtained was dried at 150°C to obtain n-HApCs composite [38, 39].

Sorption Experiments: Sorption isotherm and kinetic experiments were performed by employing the batch method by mixing 0.1 g of the sorbent with 50 m of $K_2Cr_2O_7$ solution containing an initial concentration of 10 mg/ Cr(VI) ions. The mixture was shaken at room temperature in a thermostatic shaker at a speed of 200 rpm. The Cr(VI) ion removal studies were conducted with a fixed dosage and initial Cr(VI) ion concentration in order to optimize various experimental conditions such as contact time, pH and the influence of competitor anions. Kinetic studies were carried out in a temperature controlled mechanical shaker. The effect of different initial Cr(VI) ion concentrations, viz. 8, 10 and 12 mg/L, at three different temperatures, viz. 303, 313 and 323 K, on the sorption rate was studied by maintaining the sorbent mass at 0.1 g, the solution volume at 50 m and the pH at a value of 4. The final Cr(VI) ion concentration in the aqueous solution was measured by means of a UV-vis spectrophotometer (Perkin-Elmer Lambda 35) at 540 nm (APHA 2005). All pH measurements were carried out using an Orion Research EA 940 expandable ion analyzer fitted with a pH electrode. All other water-quality parameters were analyzed by standard methods [15].

Analysis: The prepared sorbents were characterized by Fourier-transform infrared spectrometry (FT-IR). Thus, FT-IR spectra of the pelleted solid samples diluted with KBr were recorded via a JASCO460 plus instrument. The FT-IR data were used to confirm the functional groups present before and after Cr(VI) ion sorption onto the sorbents. Elemental spectra were obtained using a Hitachi S-3400 model energy dispersive X-ray analyzer (EDXA) which allowed qualitative detection and localization of the elements in the composites. The specific surface areas of the composites were obtained via a Micromeritics Tristar 3000 model instrument. Computations were made using Microcal Origin (Version 6.0) software. The goodness-of-fit was discussed in terms of the regression correlation coefficient (r), ÷2 -analysis and the standard deviation (sd).

RESULTS AND DISCUSSION

Characterization of Sorbents: The traces a-c in Figure 1 depict the FT-IR spectra of n-HAp, chitosan and n-HApCs composites, respectively. In trace a, the stretching vibrations at 632 and 3140 cm^{-1} may be attributed to the hydroxy groups in n-HAp. The bands at 560-610 cm^{-1} and 1000-1100 cm^{-1} in n-HAp correspond to PO_4^{-3} stretching vibrations [40, 41] . The peak at 1630 cm^{-1} may be due to water. In trace b, the band at 1636 cm^{-1} is due to the C=O group of chitosan in the composite. Similarly, in traces b and c, the bands at 3140 and 1634 cm^{-1} correspond to the -NH group of chitosan. The bands at 2850, 1460 and 1383 cm^{-1} may be attributed to the vibration of the -CH g roup of chitosan, although the limited intensity of this band could indicate that the -CH group content of chitosan was very small. The vibration bands of C-O group are overlapped by phosphate bands in the spectral range 1150-1040 cm^{-1} [37, 38]. EDXA methods were employed to establish whether the electron-dense portions of the composites surfaces were composed of Cr(VI) ions. The EDXA spectra of the chitosan composites depicted in Figures 2(a) and (b) confirm the presence of ions in the composites.

The quantitative elemental compositions of the composites are listed in their respective figures. That Cr(VI) ion sorption occurred onto the composites is confirmed by the presence of Cr peaks in the EDXA spectra of the Cr(VI) ion- treated composites, with the quantitative elemental composition of each composite after Cr(VI) ion sorption being listed in Figures 2(c) and (d), respectively. The characteristics of the n-HApCs composite, for example, were particle size = 80 nm, density = 0.61 g/cm3 and BET surface area = 40.07 m2 /g.

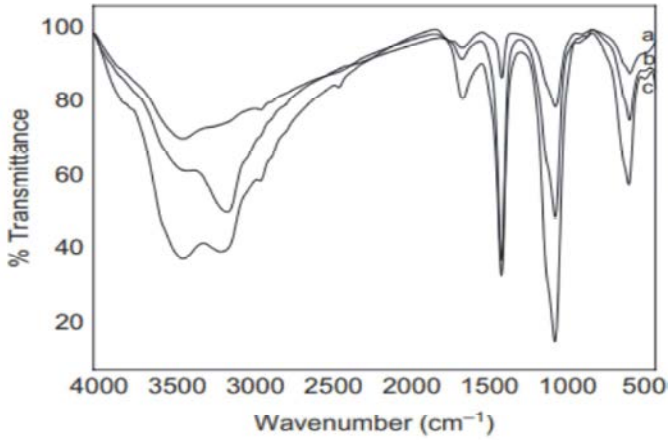

Fig. 1: FT-IR spectra of (a) n-HAp, (b) chitosan and (c) n-HApCs composite, respectively

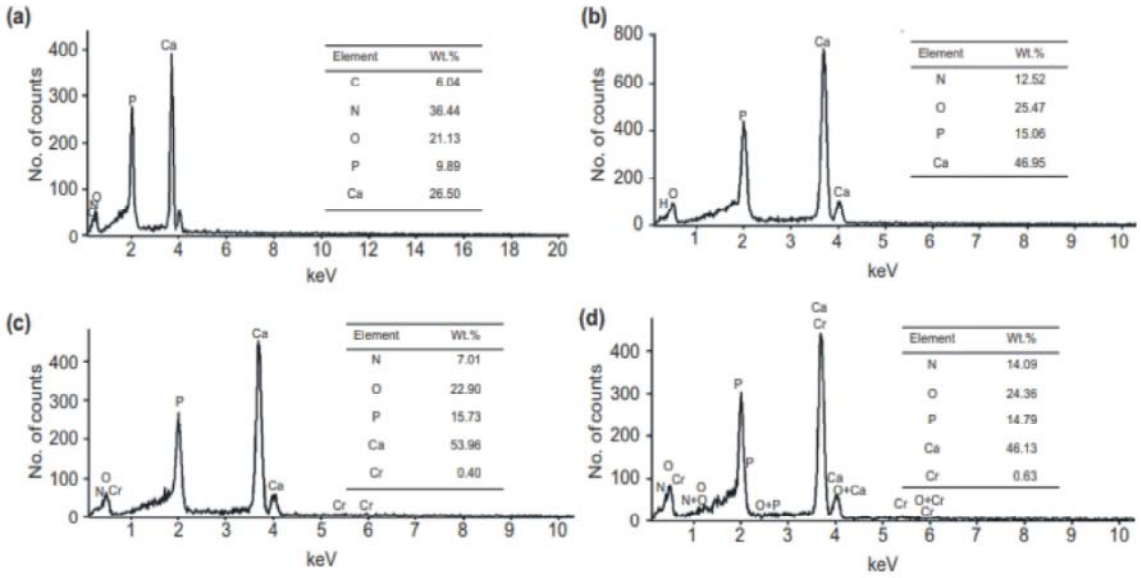

Fig. 2: EDXA spectrum of (a) chitosan, (b) the n-HApCs composite; (c) chitosan after Cr(VI) ion sorption and (d) the n-HApCs composite after Cr(VI) ion sorption

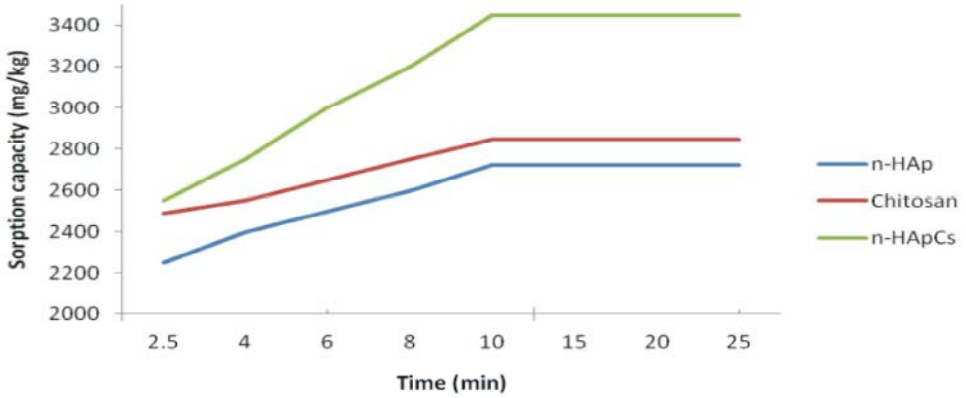

Fig. 3: Effect of contact time on the sorption capacity of n-HAp, chitosan and n-HApCs composite towards Cr(VI) ions from aqueous solution

Effect of Contact Time: As stated above, the sorption capacities of the sorbents were determined by batch methods varying the contact time between the adsorbent and the Cr(VI) ion solution within the range 5-60 min. Thus, ca. 0.1 g of the sorbent was placed into a set of six iodine flasks of 250 m capacity. Then, 50 m of the stock Cr(VI) ion solution having an initial chromium concentration of 10 mg/l was added to each flask. The contents of all six iodine flasks were shaken thoroughly using a mechanical shaker at 200 rpm. The flasks were then removed from the shaker, the contents filtered and the filtrates analyzed for their Cr(VI) ion content. As is evident from the data depicted in Figure 3, the sorption capacities of all the sorbents attained a saturation value after 10 min. For this reason, 10 min was fixed as the contact time for the sorbents in subsequent studies. The sorption capacities of n-HAp, chitosan and n-HApCs composites after a contact time of 10 min were found to be 2720, 2845 and 3450 mg/kg, respectively.

Effect of pH: In many cases, the removal of Cr(VI) ions from aqueous solution is highly dependent on the solution pH, as the latter alters the surface charge on the sorbent. For this reason, the sorption capacities of all the sorbents were determined at five different pH levels, viz. 3, 5, 7, 9 and 11, respectively. The corresponding results are depicted in Figure 4. The data depicted show that the sorption of Cr(VI) ions onto both sorbents exhibited a maximum value at acidic rather than alkaline pH values. In acid solutions, the predominant Cr(VI) ion species in aqueous solution are $HCrO^{-}{}^{4}$ and $Cr_2O_7^{-2}$, respectively. Since the surfaces of the sorbents studied were highly protonated under acidic conditions, this would favour the uptake of Cr(VI) ions in the anionic form. With increasing pH values, the degree of protonation of these surfaces would be gradually reduced [27]. Furthermore, under such conditions, the active binding sites on the sorbent surfaces would be increasingly occupied by OH- ions and hence their adsorption capacities towards Cr(VI) ions would be diminished. In the present study, the maximum value of the sorption capacity of all the sorbents occurred at pH 4. Hence, for this reason, the pH of the medium was maintained at 4 in subsequent experiments. Since the composites possessed an enhanced sorption capacity relative to n-HAp, further studies were limited solely to the composites.

Effect of Common Ions in the Medium: The sorption capacities of the sorbents in the presence of other ions which are commonly present in water, viz. Cl^-, NO^{-3}, HCO^{3-} and SO_2^{-4}, were investigated at room temperature employing a fixed initial concentration of 200 mg/lfor these ions and using an initial Cr(VI) ion concentration of 10 mg/. As shown in Figure 5, the presence of these various co-ions had little effect on the sorption capacity of the chitosan. This confirms that the composite is still capable of removing Cr(VI) ions from aqueous solution selectively even in the presence of other co-ions. Similar results were obtained for the n-HApCs composite.

Adsorption Isotherms: To quantify the sorption capacity of the sorbents studied towards the removal of Cr(VI) ions from aqueous solution, the sorption data have been evaluated employing the two most commonly used isotherm models, viz. [30] and [10]. The corresponding Freundlich isotherms for chitosan and n-HApCs are depicted in Figures 6(a) and (b), respectively. The values of the Freundlich isotherm constants for both sorbents were calculated from the linear plots of log qe versus log Ce depicted and are listed in Table 1. That 1/n lies between 0 and 1 confirms that the adsorption conditions were favourable for both sorbents.

The values of KF listed for both sorbents increase with increasing temperature, thereby confirming the endothermic nature of the sorption process. The higher values of the correlation coefficient (r) obtained for both composites indicate the applicability of the Freundlich isotherm to the data. The respective Langmuir isotherms for chitosan and n-HApCs composites are shown in Figures 6(c) and (d), respectively. The Langmuir isotherm constants, Qo and b, for both the composites were calculated from the respective slope and intercept of the linear plot of Ce /qe versus Ce , with the corresponding data also being presented in Table 1. The higher values of r listed indicate the applicability of the Langmuir isotherm to the experimental data. That the values of Qo for both composites increase with increasing temperature again confirms the endothermic nature and temperature dependence of the sorption process. The feasibility of the isotherm can be tested by calculating the dimensionless separation constant or equilibrium parameter, RL [34]. The values of RL at different temperatures studied were calculated and are also listed in Table 1. It will be seen that these values lie between 0 and 1, indicating that the experimental conditions employed were favourable towards adsorption. The fact that the values of the correlation constant, r, for the chitosan and n-HApCs composites were higher for the Freundlich model relative to the Langmuir isotherm indicates the greater suitability of the Freundlich isotherm. This fact is further supported by the low χ^2 -values for the Freundlich isotherm listed in Table 1 [42].

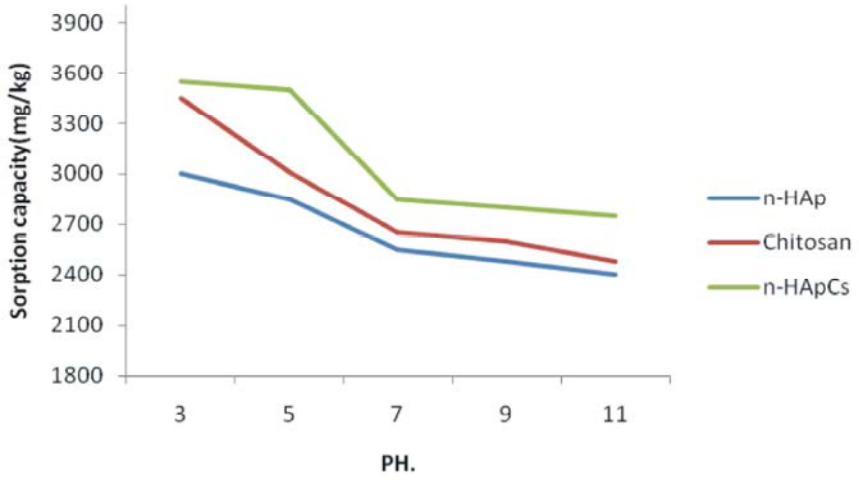

Fig. 4: Influence of pH on the sorption capacity of n-HAp, chitosan and n-HApCs composite towards Cr(VI) ions from aqueous solution at 303 K.

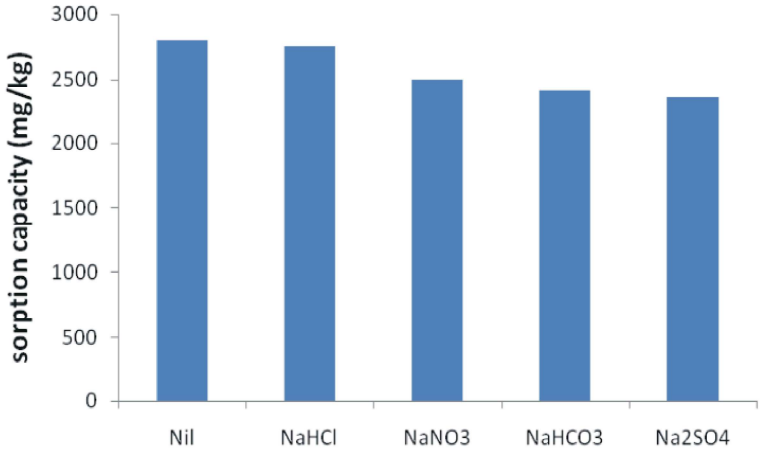

Fig. 5: Effect of co-ions on the sorption capacity of the n-HApC composite towards Cr(VI) ions from aqueous solution at 303 K.

Table 1: Freundlich and Langmuir isothermconstants for Cr(VI) ions removal by n-HApC and n-HApCs composites

Composite	Temp. (K)	Freundlich isotherm					Langmuir isotherm				
		1/n	n	K_F [(mg/(g)(ℓ/mg)$^{1/n}$]	r	χ^2	Q^o (mg/g)	b (ℓ/g)	R_L	r	χ^2
n-HApC	303	0.614	1.628	1.205	0.980	2.1E-03	7.751	0.145	0.312	0.932	2.6E-03
	313	0.613	1.631	1.479	0.967	3.9E-04	8.064	0.189	0.266	0.946	3.0E-03
	323	0.570	1.754	2.013	0.999	9.6E-05	8.403	0.274	0.230	0.995	3.4E-04
n-HApCs	303	0.643	1.555	1.538	0.999	6.8E-04	9.433	0.176	0.414	0.999	1.2E-03
	313	0.718	1.392	1.555	0.996	5.9E-04	12.406	0.127	0.361	0.967	8.7E-04
	323	0.755	3.200	1.595	0.990	4.5E-03	14.700	0.106	0.320	0.910	2.0E-02

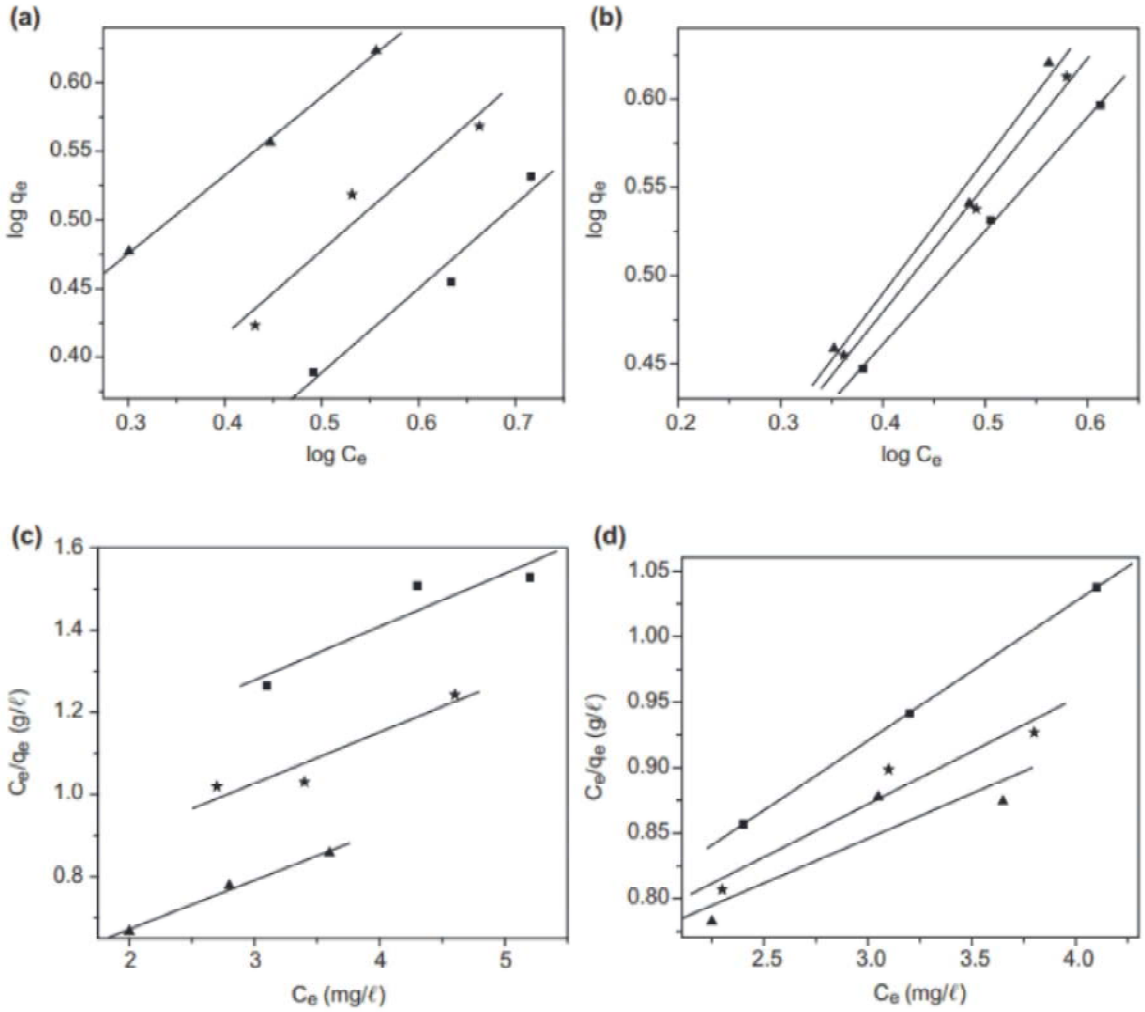

Fig. 6: Application of isotherm models to the data for the adsorption of Cr(VI) ions from aqueous solution at 303 K. (a) Freundlich isotherms for chitosan; (b) Freundlich isotherms for n-HApCs composite; (c) Langmuir isotherms for chitosan (d) Langmuir isotherms for n-HApCs composite

Sorption Dynamics: Two main types of sorption kinetic models, viz. reaction-based and diffusion-based, were employed to fit the experimental data. In this study, the initial sorbate concentration and the reaction temperature were varied in examining the influence of the sorption capacity on the rate of the reaction [43]

Reaction-Based Models: Plots of log(qe - qt) versus t were linear, thereby indicating the applicability of the Lagergren pseudo-first-order kinetic equation (1898). The values of kad and the correlation coefficient (r) computed from these plots for the chitosan and n-HApCs composites at three different temperatures, viz., 303, 313 and 323 K, are listed in Tables 2 and 3, respectively. However, the pseudo-second-order kinetic model [42] was also employed. Data-fitting and the values of qe , k and h as obtained from the plots of t/qt versus t for Cr(VI) ion sorption at the three above temperatures onto the chitosan and n-HApCs composites are presented in Tables 2 and 3. It will be seen from the tables that the qe values of the composites increased with increasing temperature, suggesting that the sorption process was temperature-dependent and thereby supporting the existence of chemisorption. The plots of t/qt versus t were linear with higher values for the correlation coefficient (r) than observed for the pseudo-first-order model. This indicates that the pseudo-second-order kinetic model was more applicable to the experimental data for the sorption of Cr(VI) ions onto both composites than the pseudo-first-order kinetic model.

Table 2: Application of kinetic models to the sorption of Cr(VI) ions onto n-HApC composite at various temperatures

Kinetic models	Parameters	At 303 K			At 313 K			At 323 K		
		8 mg/ℓ	10 mg/ℓ	12 mg/ℓ	8 mg/ℓ	10 mg/ℓ	12 mg/ℓ	8 mg/ℓ	10 mg/ℓ	12 mg/ℓ
Pseudo-first-order	k_{ad} (min^{-1})	0.481	0.417	0.396	0.416	0.400	0.373	0.262	0.409	0.398
	r	0.949	0.877	0.866	0.870	0.820	0.827	0.942	0.861	0.926
	sd	0.287	0.413	0.414	0.428	0.508	0.460	0.169	0.438	0.294
Pseudo-second-order	q_e (mg/g)	2.717	3.003	3.507	2.832	3.448	3.802	3.215	3.759	4.329
	k [g/(mg min)]	0.243	0.347	0.454	0.314	0.311	0.487	0.220	0.355	0.533
	h [mg/(g min)]	1.795	3.134	5.592	2.518	3.703	7.042	2.283	5.025	10.000
	r	0.996	0.997	0.998	0.997	0.996	0.998	0.996	0.998	0.999
	sd	0.126	0.093	0.056	0.101	0.104	0.050	0.105	0.060	0.0181
Particle diffusion	k_p (min^{-1})	0.460	0.399	0.382	0.416	0.401	0.373	0.262	0.410	0.399
	r	0.913	0.845	0.840	0.870	0.820	0.827	0.942	0.861	0.926
	sd	0.859	1.058	1.033	0.987	1.171	1.060	0.390	1.010	0.677
Intra-particle diffusion	k_i [mg/(g $min^{0.5}$)]	0.357	0.282	0.236	0.308	0.299	0.215	0.397	0.291	0.200
	r	0.992	0.993	0.991	0.995	0.969	0.976	0.995	0.988	0.996
	sd	0.036	0.027	0.026	0.024	0.066	0.040	0.032	0.037	0.014

Table 3: Application of kinetic models to the sorption of Cr(VI) ions onto n-HApCs composite at various temperatures

Kinetic models	Parameters	At 303 K			At 313 K			At 323 K		
		8 mg/ℓ	10 mg/ℓ	12 mg/ℓ	8 mg/ℓ	10 mg/ℓ	12 mg/ℓ	8 mg/ℓ	10 mg/ℓ	12 mg/ℓ
Pseudo-first-order	k_{ad} (min^{-1})	0.428	0.430	0.128	0.434	0.437	0.435	0.396	0.352	0.437
	r	0.866	0.833	0.748	0.900	0.883	0.826	0.955	0.942	0.862
	sd	0.449	0.518	0.210	0.381	0.421	0.533	0.202	0.227	0.465
Pseudo-second-order	q_e (mg/g)	3.039	3.663	3.802	3.058	3.676	4.347	3.039	3.663	4.545
	k [g/(mg min)]	0.247	0.203	0.324	0.312	0.275	0.213	0.434	0.341	0.234
	h [mg/(g min)]	2.286	2.732	4.694	2.923	3.717	4.032	4.016	4.587	4.854
	r	0.996	0.996	0.992	0.998	0.998	0.996	0.998	0.999	0.997
	sd	0.110	0.101	0.133	0.085	0.063	0.080	0.062	0.046	0.061
Particle diffusion	k_p (min^{-1})	0.428	0.431	0.130	0.434	0.437	0.430	0.452	0.384	0.603
	r	0.866	0.833	0.748	0.900	0.883	0.826	0.942	0.929	0.807
	sd	1.035	1.193	0.483	0.879	0.970	1.220	0.669	0.637	1.845
Intra-particle diffusion	k_i [mg/(g $min^{0.5}$)]	0.361	0.431	0.425	0.309	0.368	0.428	0.250	0.320	0.393
	r	0.993	0.992	0.881	0.990	0.998	0.982	0.988	0.998	0.984
	sd	0.033	0.045	0.194	0.035	0.015	0.068	0.033	0.012	0.059

Diffusion-Based Models: For a solid/liquid sorption process, solute transfer is usually characterized either by particle diffusion (kp) [38, 39]or by intra-particle diffusion control (ki) [43]. The values of kp , ki and r for the citosan and n-HApCs composites are also listed in Tables 2 and 3, where the higher values of r recorded in both cases suggest the possibility that the sorption process is also controlled by both particle and intra-particle diffusion.

The Best-Fit Model: The assessment of the fit of the sorption data by the various reaction-based and diffusion-based kinetic models was undertaken using χ^2 -analysis. In this case, lower sd values indicate a better fit to the sorption data. The sd values of all the kinetic models for both composites are summarized in Tables 2 and 3. The smaller sd values observed for the pseudo-second-order kinetic model and the intra-particle diffusion model indicate that these two models are best able to define the Cr(VI) ion sorption process on both composites. This indicates that the sorption of Cr(VI) ions occurred principally into the pores of the composites.

Mechanism of Cr(VI) Ion Sorption: The mechanism of Cr(VI) ion removal by n-HAp is governed by adsorption as well as by ion exchange, whereas both citosan and n-HApCs composites remove Cr(VI) ions via ion-exchange, complexation, electrostatic attraction and reduction steps as shown in Scheme 1. In aqueous solution, the sorbate is negatively charged and exists mainly as $HCrO_4^-$and $HCrO_7^{-2}$ anions which leads to strong electrostatic attraction between the sorbent and sorbate. However, these sorbed chromate ions are

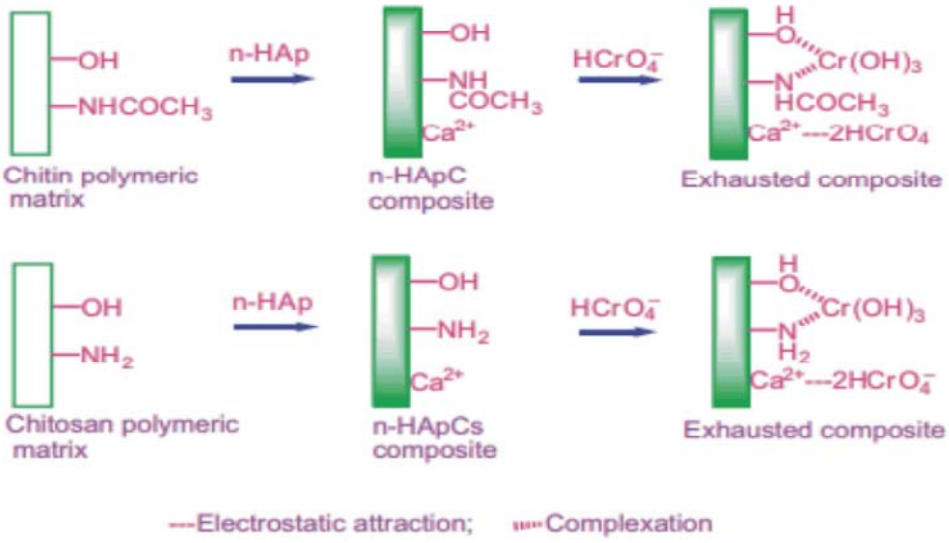

Scheme 1: Mechanism of Cr(VI) ion sorption by chitosan and n-HApCs composites

reduced to less toxic Cr(III) ions by electron-donating groups such as nitrogen and oxygen present in both bio-composites [44-46]. The higher sorption capacity of the n-HApCs composite may be due to the presence of more reactive amino groups in chitosan relative to the acetamide groups present in chitin. A comparison of the sorption capacities of the adsorbents reported in the literature for Cr(VI) ion removal from aqueous solution relative to the behaviour of chitosan and n-HApCs composites is presented in Table 5. Both the composites possess an enhanced sorption capacity which confirms their selectivity towards Cr(VI) ions.

CONCLUSION

n-HApCs composite possesses a slightly higher sorption capacity towards Cr(VI) ions from aqueous media than chitosan which, in turn, is higher than that of n-HAp. The sorption capacities of the composites were slightly influenced by the pH of the medium and were highly selective in the presence of co-ions. The Freundlich isotherm model could be applied to the sorption of Cr(VI) ions onto both composites, the process being both spontaneous and endothermic in nature. The rate of sorption followed the pseudo-second-order kinetic model and occurred through intra-particle diffusion. These biocomposites are biocompatible, efficient and biodegradable and could provide materials which are successful in the application of adsorption technology to wastewater treatment methods.

REFERENCES

1. World Health Organization (WTO), 1996. Guidelines for Drinking Water Quality, 2nd Edn, Vol. 2. World Health Organization, Geneva, Switzerland.
2. Karthikeyan, T., S. Rajagopal and L.R. Miranda, 2007. Adsorption of Maillard reaction products from aqueous solutions and sugar syrups using adsorbent resin . J. Hazard. Mater., 144: 192.
3. Ho, Y.S., 2004. Selection of optimum sorption isotherm Carbon, 42: 2115.
4. Chen, F., Z.C. Wang and C. Lin, 2002. Preparation and characterization of nano-sized hydroxyapatite particles and hydroxyapatite/chitosan nano-composite for use in biomedical materials. Mater. Lett., 57: 858.
5. Lusvardi, G., G. Malavasi, L. Menabue and M. Saladini, 2002. Removal of cadmium ion by means of synthetic hydroxyapatite. Waste Manage., 22: 853.
6. Bailey, S.E., T.J. Olin, R.M. Bricka and D.S. Adrian, 1999. A review of potentially low-cost sorbents for heavy metals .Water Res., 33: 2469.
7. Kuriakose, T.A., S.N. Kalkura, M. Palanichamy, D. Arivuoli, K. Dierks, G. Bocelli and C. Betzel, 2004. Synthesis of stoichiometric nano crystalline hydroxyapatite by ethanol-based sol-gel technique at low temperature. J. Cryst. Growth, 263: 517.
8. Volesky, B. and Z.R. Holan, 1995. Biosorption of heavy metals. Biotechnol. Prog., 11: 235.

9. Selvi, K., S. Pattabhi and K. Kadirvelu, 2001. Removal of Cr (VI) from aqueous solution by adsorption onto activated carbon. Bioresour. Technol., 80: 87.
10. Langmuir, I., 1916. The constitution and fundamental properties of solids and liquids. Part I. Solids .J. Am. Chem. Soc., 38: 2221.
11. Morshedzadeh, K., H.R. Soheilizadeh, S. Zangoie and M. Aliabadi, 2007. Removal of chromium from aqueous solutions by lignocellulosic solid wastes, 1st Environmental Conference, Department of Environmental Engineering, Tehran University, Iran.
12. Sankararamakrishnan, N., A. Dixit, L. Iyengar and R. Sanghi, 2006. Removal of hexavalent chromium using a novel cross linked xanthated chitosan .Bioresour. Technol., 97: 2377.
13. Mobasherpour, I., M.S. Heshajin, A. Kazemzadeh and M. Zakeri, 2007. Synthesis of nanocrystalline hydroxyapatite by using precipitation method. J. Alloys Compd., 430: 330.
14. Oliveira, E.A., S.F. Montanher, A.D. Andrade, J.A. Nobrega and M.C. Rollemberg, 2005. Equilibrium studies for the sorption of chromium and nickel from aqueous solutions using raw rice bran. Proc. Biochem., 40: 3485.
15. APHA, 2005. Standard Methods for the Examination of Water and Waste Water, American Public Health Association, Washington, DC, U.S.A.
16. Kousalya, G.N., M. Rajiv Gandhi and S. Meenakshi, 2010b. Sorption of chromium (VI) using modified forms of chitosan beads . Int. J. Biol. Macromol., 47: 308.
17. Gerard, P., B. Ravi, M. Nicholas and J. Zhong, 2009. Synthesis and Characterization of Nano hydroxyapatite using an ultrasound assisted method, Ultrasonic Sonochemistry, 16(4): 469-474.
18. Ho, Y.S., 2006. Second-order kinetic model for the sorption of cadmium onto tree fern: a comparison of linear and non-linear methods .Water Res., 40: 119.
19. Earl, J.S., D.S. Wood and S.J. Milne, 2006. Hydrothermal synthesis of hydroxyapatite, J. Phys. Conference Series., 26: 268-271.
20. Alessandra, B., C. Ilaria, L. Mariangela, M. Laura and G. Gusmano, 2007. Thermal stability and sintering Behaviour of Hydroxyapatite Nanopowder, J. Therm. Anal. Calorim., 88(1): 237-243.
21. Adzila, S., I. Sopyan and M. Hamdi, 2011. Synthesis of Hydroxyapatite through Dry Mechanochemical Methodand Its Conversion to Dense Bodies:
22. Preliminary Result, IFMBE Proceedings, 2011. Kinetic model for the sorption of cadmium onto tree fern: a comparison of linear and non-linear methods.
23. Nithiya, S., L. Kavitha, U. Kmchi and K. Kanimozhi, 2013. Influence of surfactant concentration on nano hydroxyapatite growth. Bull. Mater. Sci., 36(5): 799 -805 .
24. Jianping, Z., K. Deshuang, Z. Yin, Y. Nengjian and Q. Yaqiu, 2011. The Influence of Conditions on Synthesis Hydroxyapatite By Chemical Precipitation Method, Mater. Sci. Eng., pp: 18.
25. Tailored Zeolites, 47th Purdue Industrial Waste Conference Proc., Lewis Publishers Inc, Chelsea, MI, U.S.A., pp: 669.
26. Khelendra, A., S. Gurubhinder, P. Devandra and P. Satya, 2011. synthesis of hydroxyapatite powder by sol-gel method for biomedical application, J. Mater. Charac. Eng., 10(8): 727-734.
27. Gao, H., Y. Liu, G. Zeng, W. Xu, T. Li and W. Xia, 2007. Fabrication of carbon nanotubes/poly (1, 2-diaminobenzene) nanoporous composite via multipulse chronoamperometric electropolymerization process and its electrocatalytic Sensors and Actuators B. J. Hazard. Mater., 150: 446.
28. Kousalya, G.N., M. Rajiv Gandhi, C. Sairam Sundaran and S. Meenakshi, 2010a. Synthesis of nano-hydroxyapatite chitin/chitosan hybrid biocomposites for the removal of Fe (III) Carbohydrate Polymers, 82: 594.
29. Aldona, B., B. Irma and K. Aivaras, 2006. Calcium acetylacetonate-a novel calcium precursor for sol-gel preparation of $Ca_{10}(PO_4)_6(OH)_2$. Chemija, 17(2-3): 16-20.
30. Freundlich, H.M.F., 1906. Characteristics of heavy metals. J. Phy. Chem. Z. Phys. Chem., 57A: 385.
31. Argun, M.E., S. Dursun, C. Ozdemir and M. Karatas, 2006. Removal of heavy metal ions using chemically modified adsorbents. J. Hazard. Mater., 141: 77.
32. Sedlak, D.L. and P.G. Chan, 1987. Reduction of hexavalent chromium by ferrous iron. Geochim. Cosmochim. Acta, 61: 2185.
33. Sairam, S.C., N. Viswanathan and S. Meenakshi, 2008b. Uptake of fluoride by nano-hydroxyapatite/chitosan, a bioinorganic composite .Bioresource technology . J. Hazard. Mater., 155: 206.
34. Pettine, M., L. D'Ottone, L. Companella, F.J. Millero, and R. Passino, 1998. The reduction of chromium (VI) by iron (II) in aqueous solutions. Geochim. Cosmochim. Acta, 62: 1509.

35. Sairam, S.C., N. Viswanathan and S. Meenakshi, 2008a. Defluoridation chemistry of synthetic hydroxyapatite at nano scale: equilibrium and kinetic studies .Bioresour. Technol., 99: 8226.
36. Weber, T.W. and R.K. Chakravorti, 1974. Pore and solid diffusion models for fixed-bed adsorbers .AIChE J. Am. Inst. Chem. Eng., 20: 228.
37. Sheha, R.R., 2007. Sorption behavior of Zn (II) ions on synthesized hydroxyapatites . J. Colloid Interface Sci., 310: 18.
38. Li, Q., J. Zhai, W. Zhang, M. Wang and J. Zhou, 2007. Kinetic studies of adsorption of Pb (II), Cr (III) and Cu (II) from aqueous solution by sawdust and modified peanut husk '.J. Hazard. Mater., 144: 163.
39. Sairam, S.C., N. Viswanathan and S. Meenakshi, 2009. Defluoridation of water using magnesia/chitosan composite. J. Hazard. Mater., 163: 618.
40. Park, D. and J.M. Park, 2006. Mechanisms of the removal of hexavalent chromium by biomaterials or biomaterial-based activated carbons J. Hazard. Mater., 137: 1254.
41. Mor, S., K. Ravindra and N.R. Bishnoi, 2007. Adsorption of chromium from aqueous solution by activated alumina and activated charcoal .Bioresour. Technol., 98: 954.
42. Torresdey, J.L.G., K.J. Tiemann and V. Armendariz, 2000. Characterization of Cr (VI) binding and reduction to Cr (III) by the agricultural byproducts of Avena monida (Oat) biomass. J. Hazard. Mater., 80: 175.
43. Rajiv Gandhi, M., N. Viswanathan and S. Meenakshi, 2010. Reparation and application of alumina/chitosan biocomposite. Int. J. Biol. Macromol., 47: 146.
44. Sandrine, B., N. Ange, B. Didier, C. Eric and S. Patrick, 2007. Removal of aqueous lead ions by hydroxyapatites: equilibria and kinetic processes . J. Hazard. Mater., 139: 443.
45. Smiciklas, I., S. Dimovic, I. Plecas and M. Mitric, 2006. Removal of Co2+ from aqueous solutions by hydroxyapatite . Water Res., 40: 2267.
46. Vega, E.D., J.C. Pedregosa, G.E. Narda and P.J. Morando, 2003. Removal of oxovanadium (IV) from aqueous solutions by using commercial crystalline calcium hydroxyapatite. Water Res., 37: 1776.